

Minimally invasive *in vivo* human lung tissue bioimpedance measurements during the bronchoscopy procedure

B Sanchez, G Vandersteen, I Martin, D Castillo, A Torrego, P J Riu, J Schoukens and R Bragos

Abstract—Respiratory diseases, which include diseases of the lung, pleura, bronchial tree, trachea, upper respiratory tract and of the respiratory muscles and nerves, are a common and important cause of illness and death among the population. Experimental evidences have shown that tissue lesions have different electrical properties compared with normal tissue. Therefore, lung tissues lesions may be differentiated from lung normal tissue by comparing the tissue passive electrical properties. The manuscript reports a feasibility study for minimally invasive *in vivo* human lung tissue tetrapolar bioimpedance measurements using a catheter during the bronchoscopy procedure based on multisine Electrical Impedance Spectroscopy (EIS) at 10 kHz - 1 MHz.

I. INTRODUCTION

The electrical impedance of a biological material is known as Electrical Bioimpedance (EBI). It refers to the opposition that a biological material has to the flow of an electric current. In biological tissues, the electrical conductivity and permittivity varies between tissue types likewise depending on physiological factors. Through *in vivo*, *ex vivo* and *in vitro* experimentation, tissue electrical bioimpedance has been shown to correlate with many physiological states of the tissue.

The possible techniques for measuring EBI measurements is based on frequency-sweep Electrical Impedance Spectroscopy (EIS), which is a well-known widespread technique with several medical applications such as body composition determination, skin cancer detection and Electrical Impedance Tomography (EIT) among others. In contrast to the frequency-sweep EIS approach, measuring with broadband signals, i.e. multisine excitations, enables to collect simultaneously multiple lung tissue impedance data at several frequencies. However, this result is not straightforward if a frequency sweep approach is considered. In the case of the electrical properties of *in vivo* time-varying organs, i.e. the lungs, the way to overcome the main limitations imposed by sweeping the excitation frequency are two: on one hand, to cause an apnea to the patients, which is not always possible

This work has been supported in part by the Spanish Ministry MICINN SAF2011-30067-C02-02, by the Redes de Investigacion del Instituto de Salud Carlos III (REDINSCOR, RD06/0003) and Fondo Europeo de Desarrollo Regional (FEDER), by the Fund for Scientific Research (FWO-Vlaanderen), by the Flemish Government (Methusalem), and by the Belgian Government through the Interuniversity Poles of Attraction (IAP VI/4) Program.

J. Schoukens and G. Vandersteen are with the ELEC Department, Vrije Universiteit Brussels (VUB), 1050, Brussels, Belgium.

I. Martin, D. Castillo, A. Torrego are with the Respiratory Service, Hospital Santa Creu i Sant Pau (HSCSP), 08025, Barcelona, Spain.

B. Sanchez, P. J. Riu and R. Bragos are with the Departament d'Enginyeria Electronica, Universitat Politecnica de Catalunya (UPC), 08034, Barcelona, Spain. benjamin.sanchez@upc.edu

because the patient is unable to maintain the apnea as long as it takes to the system to perform the frequency sweep and, on the other hand, to perform a synchronous averaging during several ventilation cycles for noise filtering. In this case, there is the added difficulty that the patient should keep a regular ventilation. In any case, the bronchoscope time and complexity of the procedure would be significantly increased. All the mentioned reasons justify the use of the broadband EIS approach, that overcomes the previous limitations and enables to measure lung bioimpedance with enough temporal resolution due to the reduced measuring time.

In the majority of cases, lung diseases are diagnosed after the appearance of symptoms and a radiological study (usually by Computed Tomography (CT)) showing a pulmonary lesion (see Figure 1). Although the symptoms and radiological tests results may indicate the presence of the lesion, the diagnosis needs histological analysis for confirmation and cell type identification. The cells from lungs are usually obtained from sputum or by more invasive procedures such as biopsy. Due to the uncertainty in the biopsy, it is necessary to repeat this step until several samples are collected for tissue analysis. Thus, a non-destructive and minimally invasive technique like the one presented in the manuscript has a clear potential to obtain information of tissue properties helping or guiding the bronchoscopy procedure.

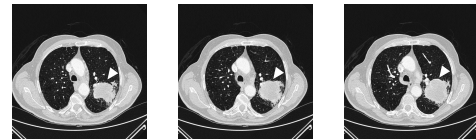


Fig. 1. Computed Tomography (CT) scanning images at different positions of the chest corresponding to patient 1467834; the white triangle indicates the presence of a cancerous mass in the left lung (right side of the image).

This manuscript describes the first steps towards minimally invasive *in vivo* human lung tissue characterization using a tetrapolar catheter during bronchoscopy procedures measured at 10 kHz - 1 MHz based on multisine Electrical Impedance Spectroscopy. For minimally invasive we mean that no incision was necessary to be performed to the patients to make the measurements so experiments were carried out in the bronchoscopies room. The aspects concerning to the design of the multisine excitation and the impedance signal processing are detailed in [1], [2] respectively. The reader is referred to [3] for a detailed description of the measurement system characterization and calibration. Additionally to the calibration and the characterization process, the accuracy of the custom measurement system is analyzed. Finally, the

modeling of the time-varying lung bioimpedance data can be found in [4].

II. MATERIALS

We employed a tetrapolar probe catheter (Bard Electrophysiology VIKING, 400041) with 115 cm length and a diameter of 1.65 mm (5F). The probe has a line of isolated polymer with four platinum electrodes separated by a distance of 2 mm and placed in the distal shaft section. For safety reasons, an isolated patient front-end previously designed to accomplish the safety regulation for medical devices (EN 60601-1) was used. The measurement system is composed by three devices:

- 1) the isolated front end, which is an optically isolated patient interface battery power provided including two ECG channels and the impedance front end.
- 2) the core of the measurement system is a rugged PC-platform based on a PXI system (PCI eXtensions for Instrumentation) from National Instruments.
- 3) an analog-optical interface front end to connect the PXI with the front end.

The system includes an embedded controller PXIe-8130, a 2 channel high-speed digitizer card PXIe-5122 (100Ms/s, 64MB/channel, 14bits) and an arbitrary waveform card PXI-5422 (200Ms/s, 32MB, 16 bits). While the AWG (PXI-5422) generates the multisine excitation $r(t)$, the two channel digitizer (PXIe-5122) simultaneously acquires (f_s 20 MHz) voltage $v(t)$ and current $i(t)$ system response (4 periods, 20 ksamples/period).

The excitation $r(t)$ is converted into an optical signal with the optical-analog interface connected to the PXI. Then, it is converted again into an electrical signal inside the front end. The voltage $v(t)$ and current $i(t)$ signals, which are optically transmitted from the front end to the optical-electrical interface, are filtered (cut-off frequency 10 MHz) and acquired with the digitizer card. The theory for the impedance spectrum estimation is based on the Local Polynomial Method (LPM) described in [2].

III. METHODS

The flexible bronchoscope was inserted with the patient in a supine position entering through the left nose hole. Once the bronchoscope was inserted into the upper airway, the vocal cords were inspected. The bronchoscope advanced to the trachea and further down into the bronchial system. Each area was visually inspected as the bronchoscope went through it. Right and left lungs were inspected. Depending on the medical staff decision, tissue could be sampled using a biopsy (transbronchial biopsy) using real-time x-ray guidance. Experiments were approved by the institutional Ethics Committee and carried out after patient approval.

The catheter was placed inside the alveolus through the same interior channel of the bronchoscope used for the biopsy. The catheter was introduced through the bronchial tree to get into the lung parenchyma, which is composed of terminal bronchioles and alveoli, both below the catheter size and distance between electrodes, and assuming to be in

fully contact with lung tissue. Nevertheless, measures with poor electrode contact were easily detectable because they appeared as artifacts in the measured impedance.



Fig. 2. Detail of an electronic biopsy of the lung tissue; the catheter is placed inside the alveolus, in contact with the lung parenchyma (alveolar tissue) (patient 430021).

IV. DATA CALIBRATION

Considering an homogeneous and linear isotropic biological object, the bioimpedance can be related to its electrical properties, conductivity σ (Sm^{-1}) and relative permittivity ϵ_r , according to the following expression:

$$Z(\omega) = \rho^*(\omega) \frac{L}{S} = \frac{1}{\sigma^*(\omega)} \frac{L}{S} = \frac{1}{\sigma(\omega) + j\omega\epsilon_0\epsilon_r(\omega)} k \quad (1)$$

where ρ^* (Ωm) is the complex resistivity, σ^* (Sm^{-1}) is the complex conductivity, ϵ_0 is the vacuum permittivity and k (m^{-1}) is known as the cell factor. The cell factor k (see eq. 1), which depends on the geometry of the electrodes L/S and the object shape, was determined by measuring the impedance of three different physiological saline solution at $25^\circ C$ the catheter and the equipment used for the *in vivo* measurement. A three-reference calibration method was employed to determine a set of coefficients at each multisine exciting frequency to correct the load dependent errors into the measurements [5].

V. SIMULATION RESULTS

A. Finite Elements Model Simulation

The impedance measurement technique used is a four-electrode and is made available through the electrodes in the catheter. These electrodes are arranged at the end of the catheter and its configuration is as follow: LCUR, LPOT, HPOT and HCUR, respectively (see Figure 3). According to the measurement system calibration procedure, the catheter was simulated placed in the middle of the lung. In a first approach, the lung was considered to be as a cylinder. The catheter was modeled by the composition of eight piled cylinders representing each of the electrodes and the polyurethane space between them. The final assembly produced a Finite Element (FE) mesh with a limited number of elements simulated under 3D quasi-static/electric AC/DC conditions.

B. Previous work on modeling lungs bioimpedance

Following Section deals with the estimation of the bioimpedance values of lung tissue when measuring with a four-electrode technique. Simulation results were obtained from the experimental data available in literature from measurements for characterizing the electrical properties

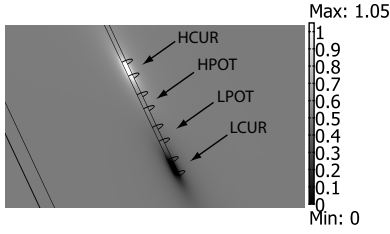


Fig. 3. Slice of the electrical potential distribution in the proximity of the electrodes of the catheter (units in Volts).

of several human tissues. The model considered describes the tissue's dielectric data as a summation of 4-Cole-Cole expression [6] using the model and the electrical conductivity σ_i and permittivity ϵ_m values available for the inflated [7] and deflated [8] lung given by:

$$\epsilon^*(\omega) = \epsilon_\infty + \sum_{m=1}^4 \frac{\Delta\epsilon_m}{1 + (j\omega\tau_m)^{1-\alpha_m}} + \frac{\sigma_i}{j\omega\epsilon_0} \quad (2)$$

where ϵ_0 is the permittivity of the free space, α is an empirical parameter characteristic of the distribution of the relaxation frequencies, τ is the characteristic time constant, σ_i the static conductivity and ω the angular frequency. For an homogeneous and isotropic linear object, the conductivity σ (Sm^{-1}) and relative permittivity ϵ_r , are complex values related according to the following expression:

$$\sigma^*(\omega) = j\omega\epsilon^*(\omega)\epsilon_0 \quad (3)$$

where ϵ_0 is the vacuum permittivity ($8.85 \cdot 10^{-12} F/m$). The complex tissue resistivity ρ^* (Ωm) is calculated as the inverse of the complex conductivity σ^* as follows:

$$\rho^*(\omega) = \frac{1}{\sigma^*(\omega)} = \frac{1}{\sigma + j\omega\epsilon_r\epsilon_0} \quad (4)$$

Considering the electrodes having negligible dimensions and being surrounded by a mass of infinite size, the lung's impedance measured with four-electrode technique can be approximated by the following expression [9]:

$$Z^*(\omega) \approx \frac{\rho^*(\omega)}{4\pi d} \quad (5)$$

where d is the distance between electrodes. For the catheter used (see Section II), the distance between the center of the electrodes is $d = 3.5mm$. With this tool in hand, Figure 4 shows the expected bioimpedance measured at 10 kHz - 1 MHz. It is possible to observe that there is a significant difference in the impedance magnitude when lungs are inflated or deflated, which is in accordance to data shown in Figure 5. The inflated lungs show a higher impedance modulus than the deflated lungs due to the fact that the electrical conductivity decreases as much as the lungs are inflated with gas. Moreover, the major phase relaxation is expected to occur close to 1 MHz in both cases, where the inflated present a lower phase value than when deflated.

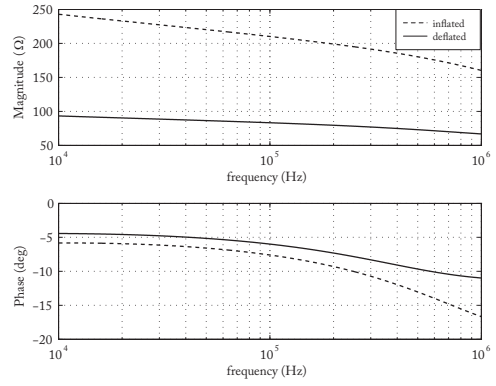


Fig. 4. Lungs inflated and deflated bioimpedance, magnitude (top) and phase (bottom), based on the model described in eq.2.

VI. PRELIMINARY EXPERIMENTAL RESULTS FROM *in vivo* HUMAN LUNG TISSUE BIOIMPEDANCE MEASUREMENTS

A total of 9 patients (7 male, 68.1 ± 15.0 years and 2 female, 64.0 ± 5.7 years) were measured both in the right and left inferior, middle and superior lung lobes respectively. The multisine fundamental frequencies were distributed as follows 10, 13, 17, 21, 26, 32, 39, 48, 59, 72, 87, 105, 186, 224, 270, 325, 391, 470, 565, 679, 816, 981 (kHz).

As it can be observed in Figure 5, the lungs bioimpedance varies with time due to the influence of the cardiac-cycle in the lungs blood perfusion, and the breathing cycle because of the lungs ventilation. An alternative to multisine EIS based on frequency-sweep EIS technique would fail to determine the impedance spectrum with enough temporal resolution due to its relatively long measuring time (around 20 seconds). In practice, this means that to be able to correctly interpret changes in the impedance spectrum, it should be synchronously averaged to avoid the influence of both the ventilatory and the cardiac signals. In addition to the inconvenience to patients due to lengthen the time of bronchoscopy, this restriction causes great practical drawbacks during the clinical experimentation. Several ventilation should be averaged and, in most of the cases, patients present difficulties to maintain breathing at a steady pace thus requiring a biofeedback system during the bronchoscopy procedure. Even then, keep breathing steadily during the bronchoscopy is not easy.

Figure 6 illustrates an example of the measurement from lungs bioimpedance spectrum. The accuracy on the bioimpedance measurement is shown by means of the impedance spectrum Signal-to-Noise Ratio (SNR_Z), defined in [10] as the difference in dB from the impedance magnitude Z and variance σ_z^2 . The SNR_Z is above 55 dB at all the multisine excitation frequencies. As shown in the Figure 6, the impedance spectrum phase is sensitive to the impedance electrode and the effective coupling between patient-catheter, introducing errors at low and high frequencies.

VII. CONCLUSIONS

Based on the preliminary experimental results presented, it is feasible and safe to measure and characterize *in vivo*

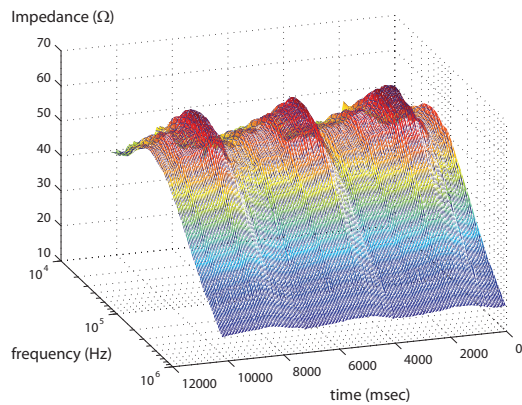


Fig. 5. Bioimpedance frequency response (dependences of modulus) as a function of the frequency and time of the *in vivo* human lung tissue (Right Superior Lobe) (patient 228209). The time resolution is 20 impedance spectra / second (24 multisine fundamental's frequencies).

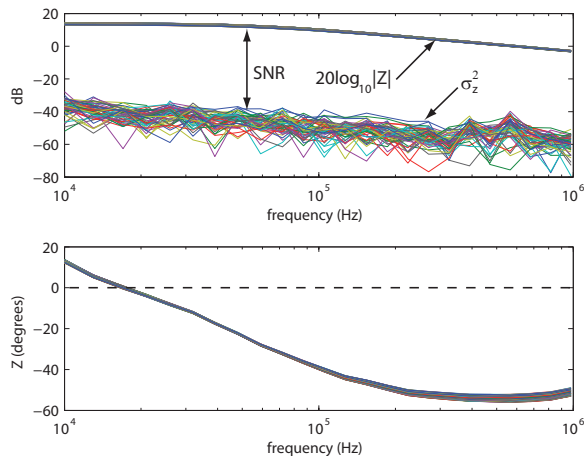


Fig. 6. Lungs tissue bioimpedance frequency response magnitude and impedance variance σ_z^2 (top) and phase (bottom) from healthy Left Inferior Lobe (LIL) lung sample (patient 1150728). The accuracy of the impedance spectrum is provided by means of the impedance SNR_Z .

human lung tissue. There were no side effects associated with the measurements of lungs bioimpedance. The lungs bioimpedance is significantly larger when inflated than deflated which is in accordance with already published data. However, the reader must be aware that the model simulated was obtained by the authors in [7] from *ex vivo* measurements, mostly within 2 hours of the animals death, and from bovine origine. Then, the validity for describing our *in vivo* human lung tissue measurements is questionable due to differences between species and due to the significant structural changes (sell swelling) during an ischemic process in *ex vivo* tissues [11]. This is probably the reason why the magnitudes of impedance differ drastically between our data the model. In fact, figure 4 shows a maximum of 150 Ω difference between inflated and deflated lungs while figure 5 shows a maximum of approximately 10 Ω . Despite the mentioned limitations, the comparison between the experimental data presented in this paper and the corresponding data from the

literature given in Section V-B shows good agreement.

With regard the FEM simulation, the goodness of FEM data depends on the accuracy of the model considered, and the one used still has some practical limitations for simulating the experimental measurements. It is necessary the construction of lung models that include pulmonary lobules within the intra-pulmonary bronchioles and also the connective tissue that binds lobules, vessels and bronchioles in order to validate lung bioimpedance data. Lungs tissue anisotropy and the spatial mapping of their electrical properties, during the pulmonary ventilation ought to be accounted for.

The technique of EIS based on multisine excitations opens up the possibility of measuring the time-varying biological tissues and organs, including the information of the time dependences. For the case of measuring the human lung tissue, provides enough time resolution and accurate impedance SNR_Z without needing to increase the bronchoscopy time neither causing discomfort to patients. Therefore, it has a clear potential interest to be used as a complementary tool for the diagnosis of lung diseases in the clinical daily practice.

REFERENCES

- [1] B. Sanchez, G. Vandersteen, R. Bragos, and J. Schoukens, "Optimal multisine excitation design for broadband electrical impedance spectroscopy," *Measurement Science and Technology*, vol. 22, no. 11, p. 115601, Nov. 2011.
- [2] B. Sanchez, J. Schoukens, R. Bragos, and G. Vandersteen, "Novel Estimation of the Electrical Bioimpedance using the Local Polynomial Method. Application to *in-vivo* real-time Myocardium Tissue Impedance Characterization during the Cardiac Cycle." *IEEE Transactions on Biomedical Engineering*, vol. 00, no. 99, pp. 1–9, 2011.
- [3] B. Sanchez, G. Vandersteen, I. Martin, D. Castillo, A. Torrego, P. J. Riu, J. Schoukens, and R. Bragos, "In vivo electrical bioimpedance characterization of human lung tissue during the bronchoscopy procedure. Part I: a feasibility study," *Medical Engineering & Physics*, no. submitted, 2012.
- [4] B. Sanchez, A. S. Bondarenko, G. Vandersteen, I. Martin, D. Castillo, A. Torrego, P. J. Riu, J. Schoukens, and R. Bragos, "In vivo electrical bioimpedance characterization of human lung tissue during the bronchoscope procedure. Part II. Parametric modeling," *Medical Engineering & Physics*, no. submitted, pp. 1–26, 2012.
- [5] J. Z. Bao, C. C. Davis, and R. E. Schmukler, "Impedance spectroscopy of human erythrocytes: system calibration and nonlinear modeling." *IEEE transactions on bio-medical engineering*, vol. 40, no. 4, pp. 364–78, Apr. 1993.
- [6] K. S. Cole and R. H. Cole, "Dispersion and Absorption in Dielectrics I. Alternating Current Characteristics," *The Journal of Chemical Physics*, vol. 9, no. 4, p. 341, 1941.
- [7] S. Gabriel, R. W. Lau, and C. Gabriel, "The dielectric properties of biological tissues: III. Parametric models for the dielectric spectrum of tissues." *Physics in medicine and biology*, vol. 41, no. 11, pp. 2271–93, Nov. 1996.
- [8] C. Gabriel, "Compilation of the dielectric properties of body tissues at RF and microwave frequencies," Tech. Rep., 1996.
- [9] R. Herman, "An introduction to electrical resistivity in geophysics," *American Journal of Physics*, vol. 69, no. 9, p. 943, 2001.
- [10] B. Sanchez, G. Vandersteen, R. Bragos, and J. Schoukens, "Basics of broadband impedance spectroscopy measurements using periodic excitations," *Measurement Science and Technology*, no. submitted, pp. 1–25, 2012.
- [11] J. Cinca, M. Warren, A. Rodríguez-Sinovas, M. Tresànceh, A. Carreño, R. Bragos, O. Casas, A. Domingo, and J. Soler-Soler, "Passive transmission of ischemic ST segment changes in low electrical resistance myocardial infarct scar in the pig." *Cardiovascular research*, vol. 40, no. 1, pp. 103–12, Oct. 1998.